Associated conference: 5th International Small Sample Test Techniques Conference

Conference location: Swansea University, Bay Campus

Conference date: 10th - 12 July 2018

How to cite: Kazakeviciute, J., Rouse, J.P., & Hyde, C.J. 2018. The development of a novel small ring specimen tensile testing technique. *Ubiquity Proceedings*, 1(S1): 29 DOI: https://doi.org/10.5334/uproc.29

Published on: 10 September 2018

The development of a novel small ring specimen tensile testing technique

J. Kazakeviciute [1,*], J.P. Rouse [1] and C.J Hyde [1]

[1] Gas Turbine and Transmission Research Centre (G2TRC), University of Nottingham, UK, NG7 2RD;
***** Correspondence: Julija.Kazakeviciute@nottingham.ac.uk; Tel.: +44-115-748-3694

Abstract: The use of small specimens in routine testing would reduce resource requirements, however, limitations exist due to concerns over size effects, manufacturing difficulties, uncertainties related to the application of representative loading conditions, and complex interpretation procedures of non-standard data. Due to these limitations, small specimen testing techniques have been mostly applied for ranking exercises and to determine approximate or simple material parameters such as Young's modulus, creep minimum strain rate and fracture toughness. The small ring method is a novel, high sensitivity small specimen technique for creep testing and has been extended in the present work for the determination of tensile material properties. Wrought aluminium alloy 7175-T7153 was tested at room temperature at 5 different loading rates. Finite element analysis was completed to evaluate the equivalent gauge section and equivalent gauge length in order to compare uniaxial tensile testing results and small ring specimen tensile testing results. An analytical solution has also been derived in order to validate the finite element analysis. It was discovered that the finite element analysis model was suitable, validated by both experimental results and analytical solution as well as that small ring specimens can be used to acquire same stress/strain data as uniaxial specimens.

Keywords: small specimen; small ring specimen; tensile testing.

1. Introduction

Small specimen testing is a developing field as small specimens are used in situations where not enough material is available for repeat testing, such as when developing a new material, or if testing facilities are too small for full size specimens, such as when effects of irradiation are being investigated. Small specimens can be used to acquire tensile properties, fatigue properties [1], fracture properties [2], crack propagation properties [3] but most of the work has been done in acquiring creep properties from small specimen testing [4].

In general there are two main types of small specimens used for tensile testing – small punch specimen and miniaturized standard specimen. Small punch specimens are suitable for identifying yield strength and UTS [5], while miniaturized standard specimens are suitable for identifying the whole stress/strain curve including Young's modulus [1]. Small punch specimens are rather standard, with most being either square 10mm x 10mm x 0.5mm [5] or circular with a diameter between 3mm [6] and 10mm [7] and similar thickness to square specimens. The force/displacement curves of these are complicated, with many different regions representing different stages of deformation in the small punch specimen, making the data difficult to interpret. Miniaturized standard specimens vary in size from 0.5mm x 0.3mm x 0.3mm gauge section [8] to rather large but still smaller than standard. Their data is easier to understand, but they are small and difficult to handle when inserting into a testing machine and ensuring suitable alignment.

The small ring specimen was developed in 2009 by T. H. Hyde and W. Sun [9]. It was developed to obtain creep strain data and had several advantages over alternative methods, such as having a long equivalent gauge length, being self-aligning and being simple to manufacture. The main shortcoming of this specimen type is that it cannot be used to obtain tertiary creep data.

The current study was undertaken in order to discover if small ring specimens are suitable for tensile testing and if stress/strain data equivalent to uniaxial stress/strain data can be extracted from the results. The main conclusion was that for this aluminium alloy at room temperature and a wide range of loading rates, small ring specimens are suitable for tensile testing.

2. Materials and Methods

The finite element model that was used modelled $1/8^{th}$ of the small ring with two pins, taking advantage of 3 planes of symmetry with symmetry boundary conditions on each. The dimensions of the model match the dimensions of the experimental small ring setup: ring internal diameter is 9mm, external diameter is 11mm,

thickness is 2mm and diameter of the loading pin in 2.5mm. The pin was modelled as an analytical rigid body because in the experimental setup the material of the pin is significantly stiffer than the material of the ring being tested. ABAQUS FEA package was used for modelling. Geometric nonlinearity is on during the loading step, as large deformations happen.

A vertical displacement of 2mm (equivalent to displacement of 4mm during experimental testing) is applied to the reference point on the modelled pin (as show in Figure 1 (a)) in order for it to deform the small ring specimen. The displacement was chosen as it is approximately the deformation at which small rings tested under tensile loading definitely fail. The displacement rate used is 0.2mm/min, but it does not affect the results as the current model is rate independent, because the material modelled does not exhibit rate dependent behaviour.

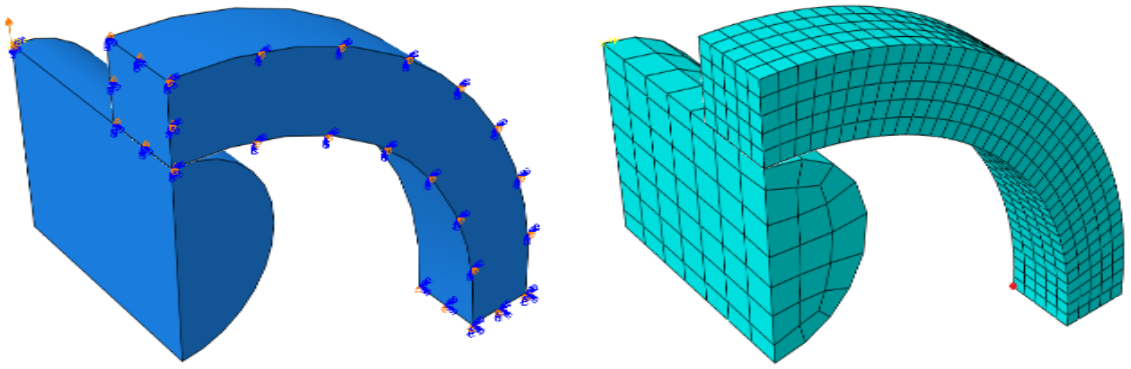

(**a**) (**b**)

Figure 1. (**a**) Loads and boundary conditions in small ring FEA model; (**b**) Mesh in the small ring and the pin model, point from which stress and strain were extracted for equivalent gauge section and length calculations highlighted in red.

Contact is defined between the pin and the ring, with the pin surface acting as a master surface because it is rigid and the surface of the ring acting as a slave surface. ABAQUS surface-to-surface contact was used with Coulomb friction. As there was no way to evaluate the coefficient of friction before this study a coefficient of friction sensitivity study was performed. It was discovered that for deformations of interest (up to 2mm in FEA), the coefficient of friction had no effect on stress, strain or reaction force on the pin when varied between minimum and maximum values of metal on metal contact therefore the model was set up with frictionless contact.

In all cases ABAQUS C3D20R elements were used for meshing. Different element types were investigated, from linear to quadratic and from 2D to 3D, this element was discovered to produce the force/displacement response of the model, the most similar to the force displacement response of experimental work. Mesh sensitivity study was undertaken to see whether the mesh was sufficiently fine to show the correct force/displacement response, but not too fine that too much computation time is spent modelling. Mesh density was uniform in the small ring specimen, where an element size of 0.2mm was used. As for the pin, the element size is larger, but it does not have a significant effect on the model outputs of interest. Both meshes can be seen in Figure 1 (b).

In order to be able to compare stress/strain data from uniaxial tests and stress/strain data calculated from small ring tensile tests, an equivalent gauge length and gauge section had to be calculated. The process was as follows: stress and strain in the y direction were extracted from the corner of the ring model (highlighted in Figure 1 (b)), reaction force and displacement in y direction were extracted from the reference point of the pin. It was determined that the shape of the force/displacement curve is due to plasticity. The FEA model was run as elastic-only and elastic-plastic, the results of both analyses can be seen in Figure 2. The initial part of the curves were determined to be elastic because the response of both models match while the next part of the curves diverged because of plasticity in the model, as nothing else was changed between the two analyses.

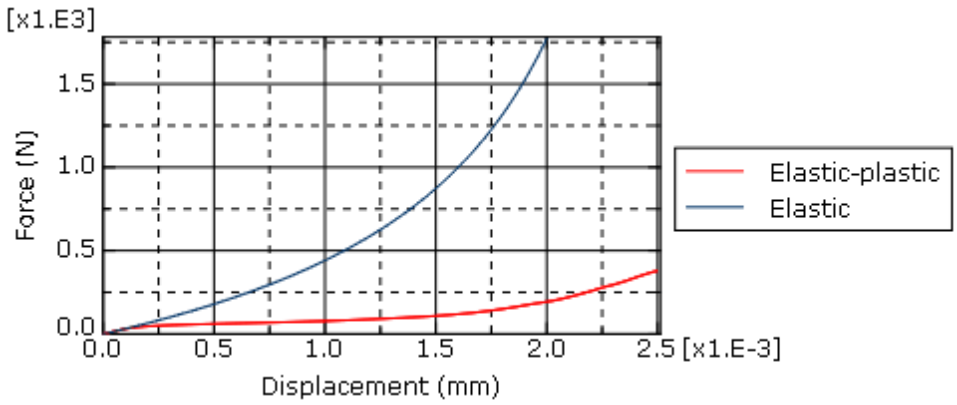

Figure 2. Comparison between elastic only material model and elastic-plastic material model response in ABAQUS.

Equivalent gauge section and length [9] were calculated using the following equations derived from the definition of strain and stress:

$$L_{gauge} = \frac{\Delta L}{\varepsilon}, \tag{1}$$

$$A_{gauge} = \frac{F}{\sigma}, \tag{2}$$

where L_{gauge} is the equivalent gauge length of the specimen, ΔL is the change in length, ε is strain, A_{gauge} is equivalent gauge section of the specimen, F is the force applied to the specimen and σ is the stress.

Material properties were acquired from uniaxial tests. As the pins are defined as analytical rigid bodies, their material properties did not need to be defined. Material was assumed to be isotropic, as previous studies show that [10].

In order to be able to use the uniaxial tensile data in ABAQUS FEA, the Ramberg-Osgood material model (deformation plasticity in ABAQUS) was fitted to it in the form of

$$\varepsilon = \frac{\sigma}{E} + \alpha \frac{\sigma}{E} \left(\frac{\sigma}{\sigma_y} \right)^{n-1}, \tag{3}$$

where E is Young's modulus, σ_y is the yield stress and α and n are constants. These model parameters were fitted to uniaxial data using Matlab Optimization toolbox. They are shown in Table 1. Poisson's ratio was determined only for one testing condition, therefore a sensitivity study was done in order to investigate the effect of Poisson's ratio on model outputs of interest. It was discovered that there is no significant effect and Poisson's ratio used was the same as experimentally determined for that one condition.

Table 1. Material parameters from Ramberg-Osgood material model.

Material	Temperature (C)	Loading rate (%/s)	E (GPa)	σ_y (MPa)	α	n
7175-T7153	RT	all	72.5	450	0.973	14.805

The material that was tested was aluminium alloy 7175-T7153, its composition can be seen in Table 2. The aluminium alloy is wrought and heat treated, specimens were machined from a hot rolled plate.

Table 2. Composition of aluminium alloy 7175-T7153 [10].

Name	Zn	Mg	Cu	Cr	Ti	Fe	Mn	Si	Other	Al
wt%	5.7	2.5	1.6	0.2	0.04	0.06	0.02	0.03	0.02	Bal

The loading rates used for uniaxial testing were 10mm/min, 1mm/min and 0.1mm/min. As the material exhibited no rate dependency at room temperature, arbitrary loading rates were chosen for small ring tensile testing. They were 60mm/min, 6mm/min, 2.04mm/min, 0.204mm/min and 0.0204mm/min.

Different machines were used to perform tensile tests. Uniaxial tests on the aluminium alloy at room temperature at 1mm/min loading rate were tested on an Instron testing machine, other loading rates were tested on a Mayes testing machine. Small ring specimens that were tested at 2.04mm/min, 0.204mm/min and 0.0204mm/min were tested on the Mayes testing machine, while others were tested on a Tinius Olsen testing machine, due to machine availability.

The analytical solution was based on a strain energy solution method. There were several assumptions made for it: the beam is slender and stress through the thickness of the ring is constant. This solution is valid for elastic behaviour only. The simplified loading situation and free-body diagram can be seen in Figure 3 (a) and (b).

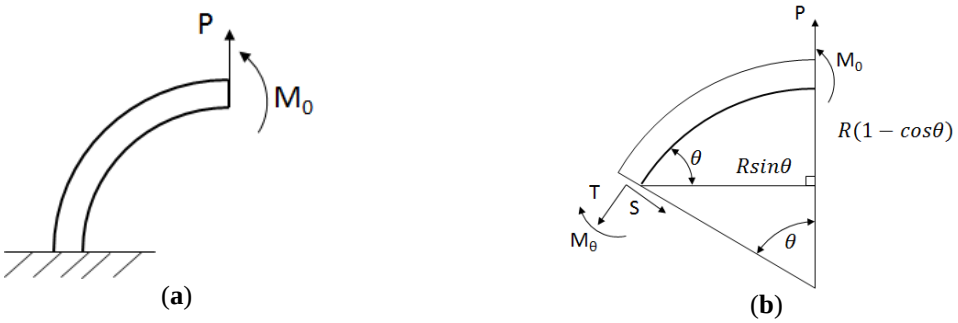

Figure 3. (**a**) Simplified loading for analytical solution; (**b**) Free-body diagram used for strain energy based analytical solution.

The moments were balanced, resulting in

$$M_\theta = M_0 + PRsin\theta, \tag{4}$$

then, according to strain energy approach,

$$U_b = \int_0^L \frac{M_\theta^2}{2EI}\, dx = \int_0^{\frac{\pi}{2}} \frac{M_\theta^2}{2EI}\, Rd\theta. \tag{5}$$

As there is no rotation caused by moment M_0, then

$$\frac{\partial U_b}{\partial M_0} = \frac{R}{2EI}\left(2M_0\frac{\pi}{2} - 2PR\right) = 0, \tag{6}$$

therefore

$$M_0 = \frac{2}{\pi} PR. \tag{7}$$

Deformation happens primarily because of bending, but there also is a tensile and shear contribution, so after balancing the force in the x and y directions and solving for T and S

$$T = Psin\frac{\theta}{2}, \tag{8}$$

$$S = Pcos\frac{\theta}{2}. \tag{9}$$

Tensile complimentary strain energy is

$$U_t = \int_0^L \frac{T^2}{2AE}\, ds = \int_0^{\frac{\pi}{2}} \frac{T^2}{2AE}\, Rd\theta, \tag{10}$$

while shear complimentary strain energy is

$$U_s = \int_0^L \frac{S^2}{2AG}\, ds = \int_0^{\frac{\pi}{2}} \frac{S^2(1+\nu)}{AE}\, Rd\theta. \tag{11}$$

As the vertical displacement of interest and it is caused by load P it is equal to

$$u_v = \frac{\partial U_b}{\partial P} + \frac{\partial U_t}{\partial P} + \frac{\partial U_s}{\partial P}. \tag{12}$$

After integrating (5), (10) and (11), then differentiating them according to (12) vertical displacement is

$$u_v = \frac{PR^3}{EI}\left(\frac{\pi}{4} - \frac{2}{\pi}\right) + \frac{PR\pi}{4AE} + \frac{PR\pi}{2AE}(1+\nu). \tag{13}$$

3. Results

Figure 4 (a) shows stress/strain results from uniaxial testing of the aluminium alloy of interest at room temperature. There is no noticeable rate dependency at these loading rates. The scatter for stress is about 50MPa. It can be seen that the Ramberg-Osgood material model does not fit very well around yield point but it fits well everywhere else. Figure 4 (b) shows the force/displacement results from small ring tensile testing of the aluminium alloy of interest at room temperature. As in uniaxial tensile testing, there is no noticeable rate dependency at these loading rates. The force scatter is about 50N. The force/displacement curves have steps in them (best seen in 60mm/min rep2).

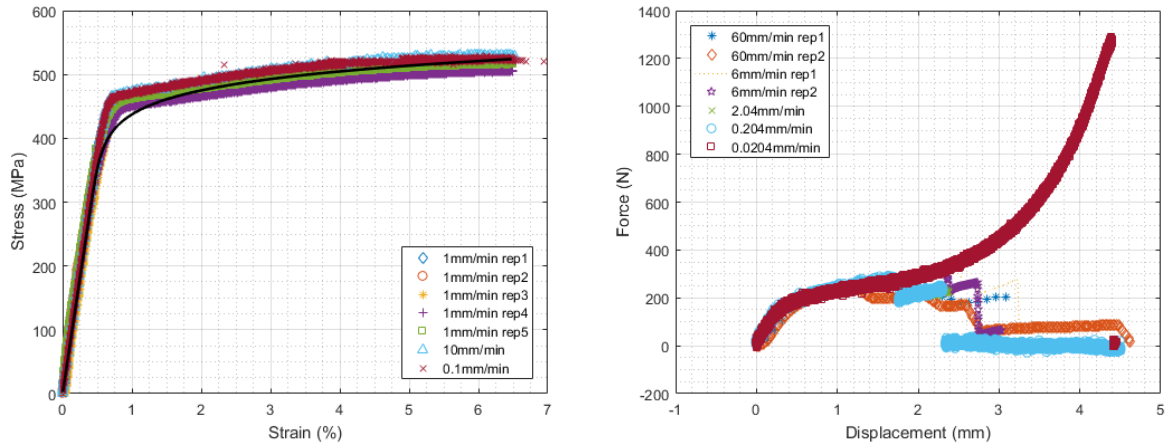

(**a**) (**b**)

Figure 4. (**a**) Collated stress/strain curves from uniaxial testing aluminium alloy at room temperature; (**b**) Collated force/displacement curves from small ring tensile testing aluminium alloy at room temperature.

Figure 5 (a) shows the equivalent gauge section, plotted against reaction force on the loading pin. The plot can be approximated to two linear regions: a horizontal one and one with a constant slope, making it simple to implement in calculating stress data from small ring tensile tests in order to compare it to uniaxial stress data. Figure 5 (b) shows the equivalent gauge length, plotted against reaction force on the loading pin. The plot can be approximated to three linear regions: a horizontal one, one with constant slope and another horizontal one, however this approximation is less accurate than the one for equivalent gauge section. This can then be used to calculate strain from the small ring tensile test in order to compare it to uniaxial strain data.

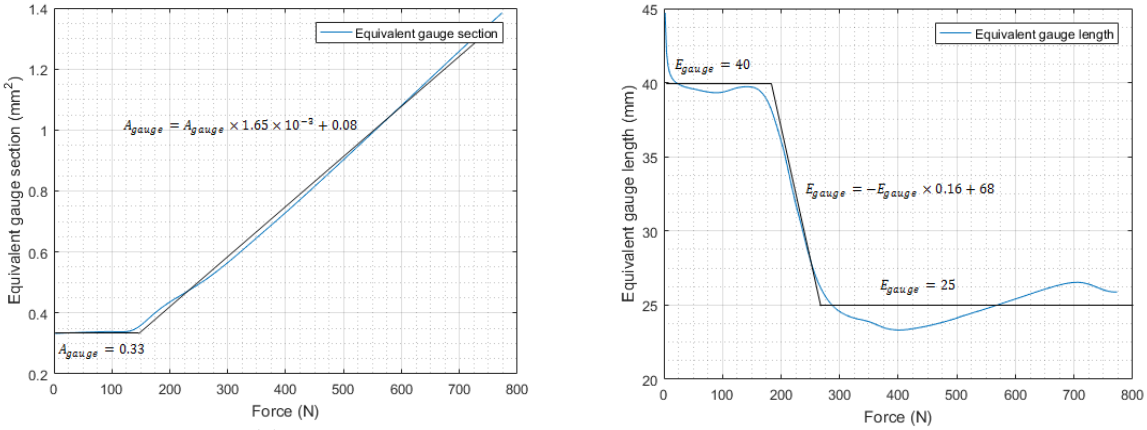

(**a**) (**b**)

Figure 5. (**a**) Equivalent gauge section, calculated from FEA plotted against force, linear approximation in black; (**b**) Equivalent gauge length, calculated from FEA plotted against force, linear approximation in black.

Figure 6 (a) shows an example of the small ring tensile data sets plotted along with ABAQUS FEA simulation equivalent and analytical solution equivalent. It can be seen that analytical solution matches FEA and experimental data well at the elastic region of the force/displacement curve then diverges. The FEA solution matches experimental data very well up to 1mm of displacement and quite well up to the first crack in the experimental data. Figure 6 (b) shows an example of how well the data matches the uniaxial tensile test results plotted along with stress/strain data calculated from one of the small ring tensile tests. It can be seen that both uniaxial and calculated data match well, apart from the region around yield.

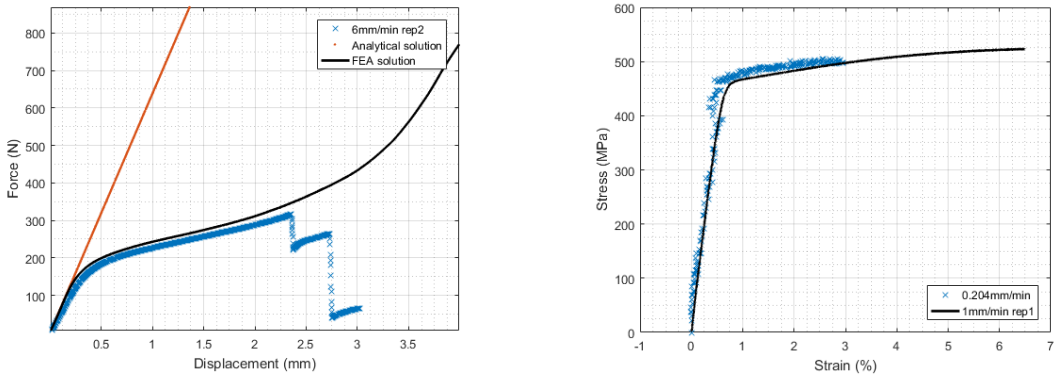

(**a**) (**b**)

Figure 6. (**a**) Small ring tensile experimental data plotted against FEA solution data and analytical solution data; (**b**) Stress/strain data from uniaxial test plotted against stress/strain data calculated from small ring tensile test data and FEA solution.

4. Discussion and Conclusions

As seen in Figure 4 (a) uniaxial test results are repeatable, which means that the material is uniform and the testing machine and methodology are suitable for this test. The Ramberg-Osgood material model does not fit well around yield because the maximum strain to which it is fitted is too high. If it was lower the model would fit around yield better. The higher strain was selected for the material model because the small ring experiences large strains during tensile testing, so representing large strains is important.

Small ring tensile testing results are also repeatable as seen in Figure 4 (b) and the material does not exhibit rate dependency, like during uniaxial testing. This means that results from small ring tensile testing and uniaxial testing can be compared. The steps in the force displacement curves are there because when the ring fails it does not usually crack through the whole thickness of the ring but instead a crack forms, the ring deforms some more and the crack grows in steps until it finally fails.

Linear approximations of equivalent gauge section and length seen in Figure 5 (a) and (b) do not represent the region around yield very well. A constant equivalent gauge section in Figure 5 (a) is in the elastic region and steadily

increasing one is in the plastic region. The part which diverges from linear approximation is around where yield first happens and is most likely there because the ring geometry and loading is quite complicated in comparison with a uniaxial specimen. The first horizontal region in Figure 5 (b) is the elastic region, latter regions are plastic.

As seen in Figure 6 (a) the FEA solution was validated by the analytical solution in the elastic region of the force/displacement curve. The FEA solution also matches experimental data well, therefore the model in FEA is suitable for modelling this test. There does not seen to be a way to implement damage mechanics into this model and get any useful results because first crack initiates over a wide range of displacement values and the number of steps in the force/displacement data also does not seem to follow a trend.

Uniaxial test results match well with calculated test results seen in Figure 6 (b), apart from the region around yield, which could be improved by using a piecewise approximation with more pieces. Even with the current approximation small ring tensile test can be used to get the similar data to uniaxial tensile testing. Maybe if inverse analysis described in [11] was used, small ring tests could be used to get uniaxial stress/strain curves.

Overall small ring specimens appear to be suitable to perform tensile tests on this material as both material and ring are isotropic. The scatter in both uniaxial and small ring tensile testing is similar when compared after adjusting the force data with equivalent gauge section.

Regarding future research, there are three main follow-up investigations that will be happening. The first one is testing this same material at elevated temperatures and developing an FEA model that can produce comparable force/displacement curves. This will most likely require the introduction of rate dependency in the model as at elevated temperature this material exhibits noticeable rate dependency. The second investigation is testing different materials, such as a steel or a nickel superalloy at various temperatures and checking if FEA and experimental data matches. If both of those are successful the third follow-up investigation is to develop a method for cyclically loading the small ring specimen in order to get fatigue data from it.

Acknowledgments: The authors wish to acknowledge Rolls-Royce plc. and EPSRC (EPSRC CDT Grant No: EP/L016206/1) in Innovative Metal Processing for financial support.

References

1. Holländer, D.; Kulawinski, D. et al. Investigation of isothermal and thermo-mechanical fatigue behavior of the nickel-base superalloy IN738LC using standardized and advanced test methods. *Mater. Sci. Eng. A* **2016**, *67*, 314-324, 10.1016/j.msea.2016.05.114.
2. Han, W.; Yabuuchi, K. et al. Application of small specimen test technique to evaluate fracture toughness of reduced activation ferritic/martensitic steel. *Fusion Eng Des* (in press).
3. Shin, C.-S.; Lin, S.-W. Evaluating fatigue crack propagation properties using miniature specimens. *Int J Fatigue* **2012**, *43*, 105-110, 10.1016/j.ijfatigue.2012.02.018.
4. Hyde, T.H.; Hyde, C.J.; Sun, W. Theoretical basis and practical aspects of small specimen creep testing. *J Strain Anal Eng Des* **2013**, *48*, 112-125, 10.1177/0309324712463299.
5. García, T.E.; Arroyo, B. et al. Small punch test methodologies for the analysis of the hydrogen embrittlement of structural steels. *Theor. Appl. Fract. Mech.* **2016**, *86*, 89-100, 10.1016/j.tafmec.2016.09.005.
6. Kumar, K.; Pooleery, A. et al. Evaluation of ultimate tensile strength using Miniature Disk Bend Test. *J Nucl Mater* **2015**, *461*, 100-111, 10.1016/j.jnucmat.2015.02.029.
7. Song, M.; Guan, K. et al. Size effect criteria on the small punch test for AISI 316L austenitic stainless steel. *Mater. Sci. Eng. A* **2014**, *606*, 346-353, 10.1016/j.msea.2014.03.098.
8. Kumar, K.; Pooleery, A. et al. Optimisation of thickness of miniature tensile specimens for evaluation of mechanical properties. *Mater. Sci. Eng. A* **2016**, *675*, 32-43, 10.1016/j.msea.2016.08.032.
9. Hyde, T.H.; Sun, W. A novel, high-sensitivity, small specimen creep test. *J Strain Anal Eng Des* **2009**, *44*, 171-185, 10.1243/03093247JSA502
10. Wing Cheong, M. F. L. Experimental and Numerical Investigations into the Behaviour of a 7175-T7351 Aluminium Alloy for Aerospace Gearbox Housing Applications at Elevated Temperatures. PhD, University of Nottingham, Nottingham, UK, 2018.
11. Husain, A.; Sehgal, D.K.; Pandey, R.K. An inverse finite element procedure for the determination of constitutive tensile behavior of materials using miniature specimen. *Comput Mater Sci* **2004**, *31*, 84-92, 10.1016/j.commatsci.2004.01.039.